Topic

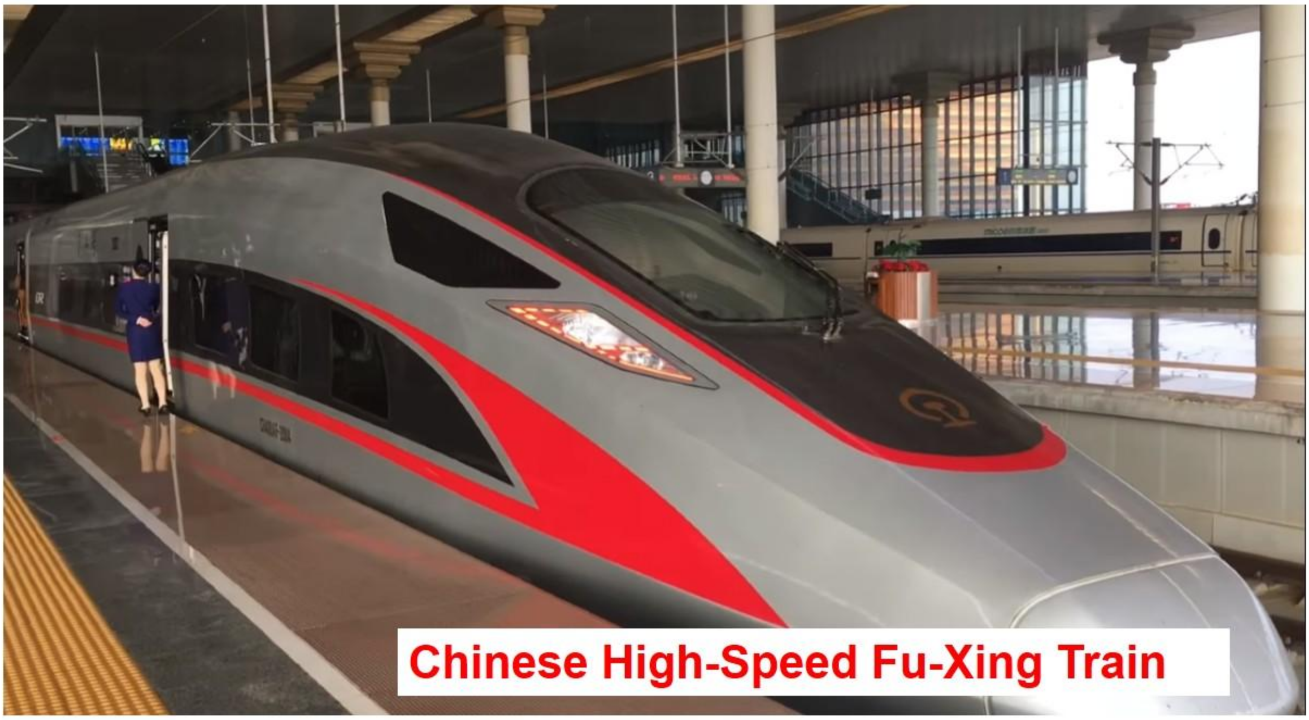

Superconducting Traction Transformer

Traction - the HTS Transformer Killer Application?

Wenjuan Song, Zhenan Jiang, Mike Staines, Stuart Wimbush, Jin Fang, Jinping Zhang, and Rod Badcock

Table of contents summary

HTS transformers are cool, sure, but are they practical? Design studies for the transformer of the Chinese Fuxing high-speed train show that an HTS transformer system can have half the weight and one tenth the losses of a conventional transformer.

Abstract

An ongoing project to develop HTS traction transformers for the Chinese Fuxing high-speed train is demonstrating that the high power density accessible using high temperature superconductors (HTS) can produce spectacular results: the existing 6.5 MVA traction transformers can be replaced with drop-in superconducting transformers which can achieve targets of less than 3 tons transformer system weight and 99.5% efficiency compared to 6 tons and 95% in the existing devices.

The key to achieving these impressive figures is minimising the AC loss of the HTS windings. New high-performance wire, high current HTS Roebel conductor, high aspect-ratio windings, and flux diverters placed at the winding ends all contribute to reducing the electrical loss to less than 2 kW.

Keywords: Traction transformer; AC loss; HTS wire; Cooling system

1. **Introduction**

High-speed rail provides an alternative to short-haul air travel with the potential for significantly reducing transportation CO_2 emissions [1]. China's high-speed rail network has developed extremely rapidly in a little over a decade, now comprising over half of the global track length and carrying more than twice as many passengers as its domestic airlines [2].

The traction transformer is a key component of high-speed trains. Fig. 1 shows the layout of the transformer system for the Chinese Fuxing train. The 6.5 MVA transformer supplies power to four drive units. With windings operating at high current density to optimize system weight, the transformer is only 95% efficient. As a result, the 300 kW oil cooling system takes a large share of the weight and space. The whole system weighs just under 6 tons.

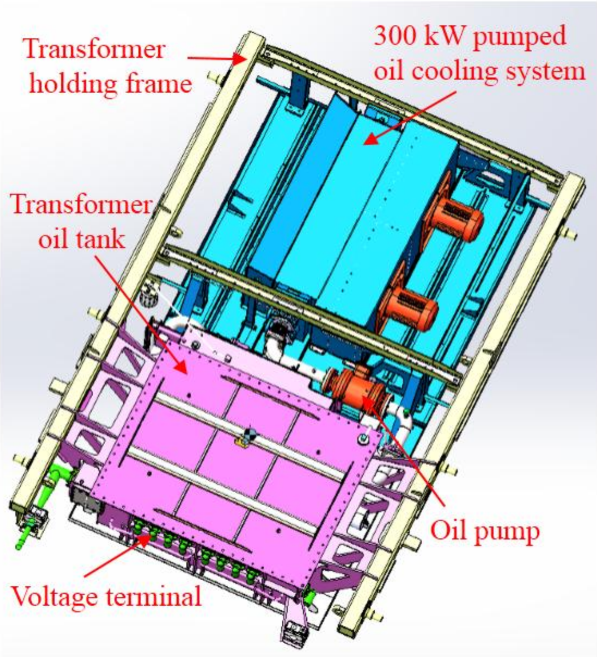

Fig. 1. Layout of conventional 6.5 MVA traction transformer for the Fuxing high-speed train.

These characteristics are typical of conventional traction transformers. There is also a significant fire hazard. These deficiencies, particularly weight, become more constraining with increasing train speed. High temperature superconducting (HTS) transformers, in contrast, offer high power density, high efficiency, and much lower fire risk thanks to their liquid nitrogen dielectric.

There have been two earlier projects aimed at demonstrating HTS traction transformers. In 2003, Siemens produced a 1 MVA traction transformer notable for the first use of HTS Roebel cable in the transformer windings [3], and about the same time the Japan Railway Technical Research Institute developed a 4 MVA HTS transformer [4]. Both of these projects used so-called first-generation wire, a bismuth strontium calcium cuprate superconducting composition. This wire has since been largely superseded for transformer applications by second-generation wire, based on thin film yttrium barium cuprate which exhibits much lower loss in the parallel ac magnetic fields which pervade transformer windings. Both transformers used liquid nitrogen as both dielectric and coolant. The Japan Rail transformer operated at 66 K, 11 K below the boiling point of liquid nitrogen. It had 7 kW loss at rated power and required a cryocooler that was bigger and heavier than the transformer itself. The efficiency of the Siemens transformer was not reported.

This article reports key findings from the design stage of an ongoing project to develop an HTS traction transformer for the Chinese Fuxing high-speed trains. The project is led by Beijing Jiaotong University, and includes manufacturing partners for the Fuxing train as well as the Robinson Research Institute, Victoria University of Wellington, which has extensive experience in HTS transformer development [5, 6].

Target specifications for the project are reduction of losses to give an efficiency of greater than 99% and reduction in total system weight, including cooling system, to under 3 tons. The system must be a drop-in replacement for the existing conventional transformer system, matching its 43% impedance, and fitting within the allocated space. The specifications are summarized in Table 1.

Table 1. Target specifications of the Fuxing HTS traction transformer.

	HV winding	LV winding
Frequency (Hz)	50	
Rated capacity (kVA)	6433	4 × 1608
Rated voltage (V)	25000	4 × 1900
Rated current (A)	257	4 × 846
Short circuit impedance	43%	
Efficiency	> 99%	
Weight (kg)	< 3000	

The key to achieving the weight reduction is minimizing the loss of the HTS windings. This is absolutely critical, because loss impacts not only on the transformer efficiency, but on the capacity and weight of the cryogenic cooling system. New high-performance wire, high current HTS Roebel conductor, high aspect-ratio windings, and flux diverters placed at the winding ends all contribute to reducing the calculated electrical loss to less than 2 kW, thereby meeting the 99% efficiency target. A compact light-weight cooling system has been designed based on open-loop cooling from an onboard liquid nitrogen storage tank rather than a closed-loop cryocooler.

In this article we describe the key characteristics of available HTS wire, the modelling to calculate ac electrical loss in the transformer windings, and the design of the cooling system to extract this heat loss from the cryostat.

2. HTS wire

High temperature superconducting wires are fundamentally different from “ordinary” (metallic) conductors, in both performance, appearance and behaviour. In the first place, they are ceramic oxides rather than simple metals. Therefore, to make them malleable as wires, they need to be “deposited” as thin films onto a carrier substrate. (Think of the way glass can be made flexible in the form of thin optical fibres; in the same way, these ceramics can be made flexible – to some degree – if applied as thin coatings to a flexible carrier.) As a result, the wires are not the usual circular cross-section, but rather thin, flat tapes of conductor.

Despite their thin film nature – typically a few microns thick on a 100 μm carrier – the amount of current these superconductors can carry is so much greater than copper that it remains 50–100 times greater when averaged across the full cross-section of the wire.

But the behaviour of the wires is very different to what we are used to with copper. In place of the Ohmic characteristic of copper wires, superconductors exhibit a power-law characteristic similar to a diode, but with current and voltage reversed. Fig. 2 plots a typical *I-V* curve of HTS wire. Equation (1) shows the highly nonlinear *V-I* power law for superconductors, where n normally varies between 20 and 30. Thus, it is essential to operate superconducting wires below the “knee” on the characteristic curve, which is termed the “critical current”, I_c. Of note, the critical current is typically of the order of hundreds of amps, equivalent to a current density of 50 kA/cm^2 in the wire as a whole or an astounding 5 MA/cm^2 in the thin superconducting layer alone.

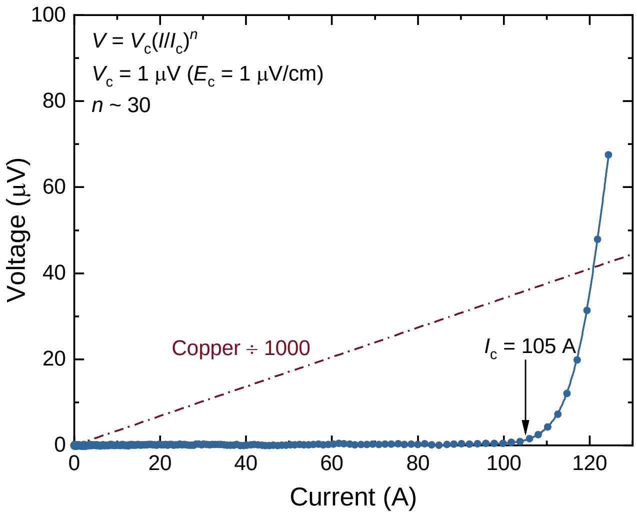

Fig. 2. Typical *I*-*V* curve of HTS wire.

$$V = V_c\left(\frac{I}{I_c(T,B,\theta)}\right)^n \tag{1}$$

However, this extreme level of performance doesn't come without complications. The current density values quoted above are best-case values based on a particular set of operating conditions, and it turns out they depend strongly and non-linearly on the temperature of the conductor, the magnitude of any magnetic field it experiences and even the precise orientation of that magnetic field. These factors are all of critical importance in the design of a transformer or any other superconducting device. Furthermore, while metallic wires are composed of a single elemental material (e.g. copper or aluminium) the superconductor is a complex quaternary compound $YBa_2Cu_3O_{7-\delta}$. While the only variation possible in a metallic wire is in the type or purity of the metal, both of which are well known to affect the electrical conductivity in predictable ways, in the superconductor minute compositional variations can lead to drastic performance variations in the wire. Indeed, most superconducting wire manufacturers intentionally introduce these variations into their product with the aim of enhancing performance under certain operational conditions, with an inevitable detrimental impact on performance under other conditions. As a result, selection of the most appropriate wire for the particular application, and qualification of wire delivery to ensure that it meets required specifications under the relevant operating conditions, becomes an essential and non-trivial undertaking.

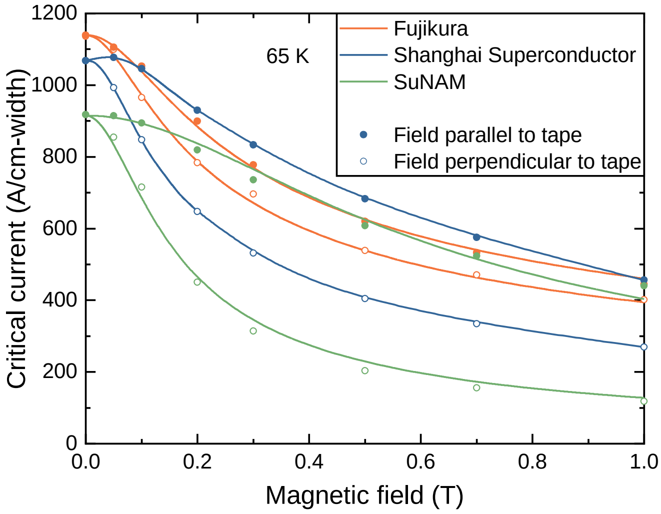

Fig. 3. $I_c(B)$ for different HTS wires, with field applied in different directions.

To outline the design process in terms of one of the simpler of these parameters, the operating temperature, we can again make the comparison to copper wires. The conductivity of copper is well known to increase with decreasing temperature. In fact, there is a factor 10 reduction in resistance, and thereby a three-fold increase in the current capacity ($P = I^2R$) of copper wires on dropping their temperature from room temperature to the common 77 K (−196°C) operating temperature of superconducting wires. (Note that this three times improvement compares poorly with the 50−100 times improvement superconductors offer over copper.) Similarly, the critical current of the superconducting wire increases approximately linearly with decreasing temperature below its critical operating temperature, T_c of around 90 K and consequently, we can approximately double the critical current of the superconductor by choosing to operate it at 65 K instead of 77 K. These slightly strange-seeming operating temperatures are determined by the melting point and the boiling point, respectively, of liquid nitrogen – a cheap, safe, non-toxic, easy-to-handle cryogenic coolant that also doubles as an excellent dielectric for the transformer, replacing the oil used in conventional transformers and its attendant fire risk in case of accident. As it turns out, this boost in performance proved to be exactly what was needed to generate a viable transformer design within the tight constraints of a traction application.

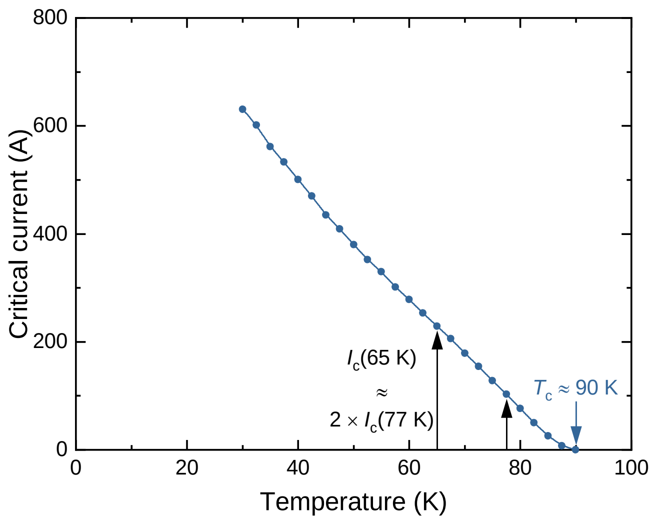

Fig. 4. Variation of superconductor critical current with temperature.

3. AC loss calculation

Superconductors have the particular advantage of supporting very high dissipation-free DC current density. Unavoidable losses do occur, however, under AC conditions due to the motion of magnetic flux within the superconductor. Loss in metallic conductors can be easily estimated because of the linear *I-V* characteristic, determined by the resistivity. In contrast, calculating the loss in HTS conductors subjected to AC current and field is not trivial. There are two main reasons for the challenge: one is the highly non-linear *I-V* characteristic of the superconductors; the other is their high aspect ratio. The thickness of the superconducting layer is normally only 1 - 2 μm, and the typical width of the tape is 4 mm or 12 mm. Therefore, the aspect ratio of a second-generation superconductor could be as large as 12,000:1. The high non-linearity makes computing convergence difficult and the large aspect ratio leads to a huge number of elements which requires long computing time.

3.1 *Numerical method of AC loss calculation*

To tackle on the computing challenges, a 2D finite element method was adopted to model and investigate superconductor behavior and calculate losses, by solving Maxwell's equations taking account into intrinsic properties of the superconductor. We established a 2D axisymmetric finite element model for the 6.5 MVA traction transformer using commercially available software COMSOL Multiphysics. Details of the modelling method can be found in [7].

Fig. 5 shows a schematic diagram of the 6.5 MVA superconducting transformer design. The transformer is composed of four winding units, with the dashed red line indicating one winding unit. Each unit is comprised of one HV and one LV winding. Two units are wound around one leg of the iron core. The transformer winding length is defined by *L*, indicated by the solid red line.

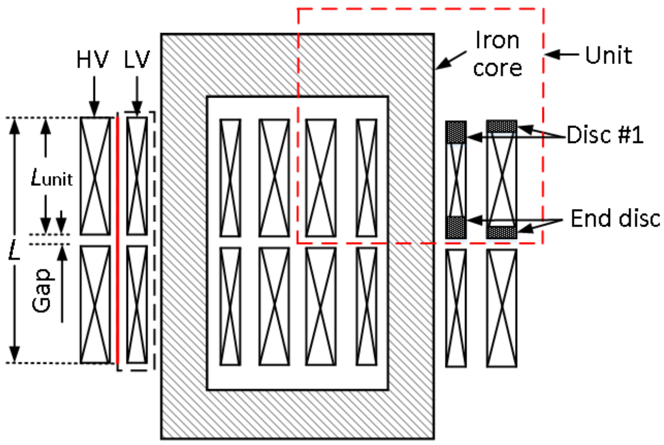

Fig. 5. Schematic diagram of the 25 kV/1.9kV 6.5 MVA traction transformer windings.

3.2 Reducing AC loss with longer windings

Ampère's law can be written as $\oint H\,dl = NI$, where *H* is the magnetic field, *l* is averaged magnetic length, and *NI* is the ampere-turns of the LV winding. Since the HV and LV windings carry opposing currents, the resulting magnetic fields will cancel out in the outer region of the HV and LV windings, whereas in the gap between these two windings, the axial magnetic field B_z reaches its strongest value as shown by the solid red line on Fig. 5.

Assuming the magnetic field along the external portion of the loop (the black dashed line in Fig. 5) is negligible, the amplitude of B_z follows the relation $B_z \approx \mu_0 NI/L$. This means B_z will be reduced when the axial winding length L is increased. Due to the continuity of magnetic field, the radial magnetic field, B_r close to the end of the LV winding should be reduced by increasing winding length L too. The same principle can be applied to the HV winding. Thus, here we propose an approach to achieve AC loss reduction in transformer windings by increasing winding length, since the AC loss in the windings is mainly determined by the B_r components in the end windings [7].

To validate the AC loss reduction approach mentioned above, AC loss calculations were conducted on three transformer winding designs with various winding lengths. As listed in Table 2, the winding lengths are 0.38 m, 1 m, and 1.5 m, designated as L038, L1, and L15. The HV windings are comprised of stacks of double pancake coils, while the LV windings are comprised of multi-layer solenoid windings wound by 8/5 (eight 5 mm-wide stranded) Roebel cables. It is noted that solenoid layer windings were regarded as disc windings in our simulation for simplicity. Two-disc windings in the LV winding are equivalent to one turn of Roebel cable, since Roebel cable was simulated as two parallel stacks of conductor.

Table 2. Specifications of winding designs with different winding lengths.

Transformer winding design label	**L038**	**L1**	**L15**
Winding length L (m)	0.38	1	1.5
Axial gap between the two units on each leg (mm)	20	20	20
Short-circuit impedance (%)	43	43	43
HV winding			
Number of turns in each disc	38	14	9
Number of discs stacked per unit	42	116	174
Total turns per unit	1596	1624	1566
Inner diameter (mm)	348	437	495
LV winding			
Number of layers of Roebel cable	8	3	2
Number of turns in one layer	15	40	60
Total turns per unit	120	120	120
Inner diameter (mm)	285	285	285

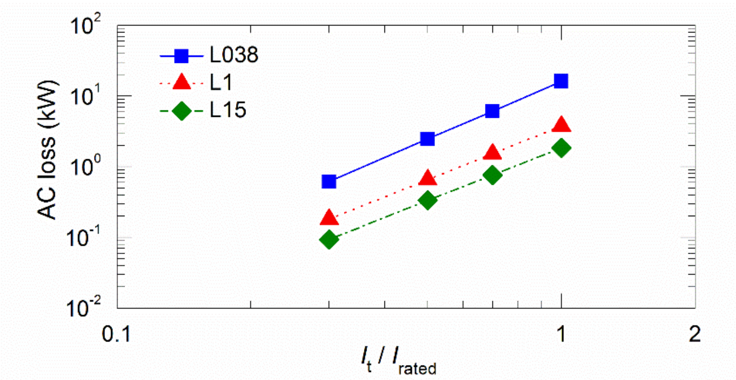

Fig. 6. AC losses in the transformer with different winding lengths. The x-axis indicates the current as a fraction of the rated current.

The computed AC losses for the whole transformer windings with different winding lengths are shown in Fig. 6. The figure shows that AC losses decrease when winding length increases. The result confirms the hypothesis in the earlier part of the article that AC loss in transformer windings can be reduced with increasing the winding length.

It is obvious that longer winding lengths lead to a longer and heavier iron core, and one might argue that large winding length is not preferable. However, shorter winding lengths will result in larger AC losses and a consequently larger cooling system, hence a greater total system weight. Although the lowest AC loss occurs in the design with 1.5 m winding length, the design with a 1 m winding length was ultimately chosen for the transformer. This is because a transformer with a longer winding length is difficult to arrange transversely to the direction of travel, making system integration difficult.

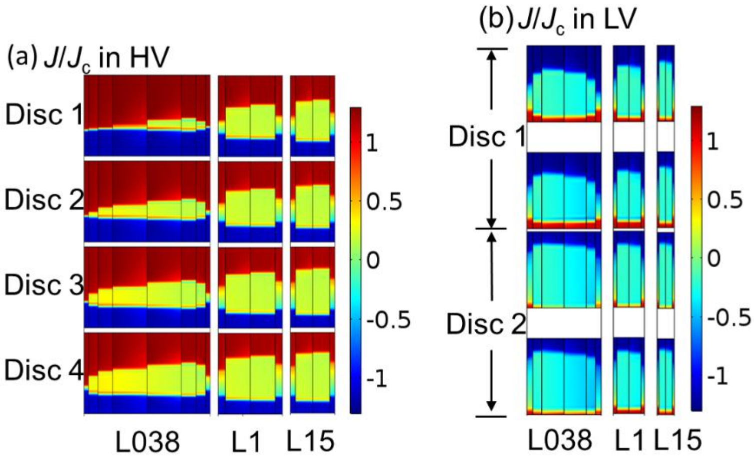

Fig. 7. J/J_c distribution in transformer windings with different winding lengths: a) HV winding, b) LV winding.

The J/J_c distribution at the uppermost discs of the HV and LV windings with various winding lengths operated at rated current is shown in Fig. 7. Current opposed to the coil current is found in all discs and shields the radial magnetic field component in the discs. In the region where $|J/J_c| > 1$, the superconductor is fully penetrated by the magnetic field and AC loss is generated in the fully penetrated region. The region where $|J/J_c| > 1$ is largest for the smallest winding length, and smallest for the largest winding length. The results reconfirm the earlier hypothesis.

3.3 High performance wire reduces the AC loss

To investigate the impact of wire performance on the AC loss of the transformer, AC loss calculations were carried out using two different characteristics for the wire $I_c(B)$ at 65 K. Wire #1 and Wire #2 are Fujikura wire and SuNam wire, respectively. The wires have same self-field I_c (915 A/cm) at 65 K, and the wire $I_c(B)$ curves are scaled from curves shown in Fig. 3.

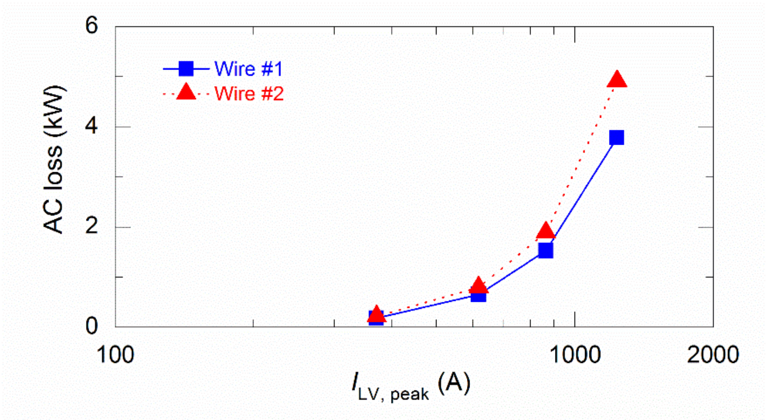

Fig. 8. Calculated AC loss in the 6.5 MVA transformer windings wound with different wires.

The AC loss values in L1 transformers wound with wire #1 and #2 are compared in Fig. 8. At rated current, wire #1 has 27% lower AC loss than wire #2. The results clearly show that the AC loss in the windings strongly depends on the critical current infield performance.

3.4 Use high performance wire only at the winding ends to reduce cost without increasing AC loss

A hybrid winding structure was proposed to achieve both low cost and low AC loss for the transformer windings by using superconductors with different $I_c(B)$ performance in different parts of the transformer windings [8]. The main idea is to use high performance wire in the end part of the windings where the radial magnetic field is the strongest, and to use relatively low performance – and therefore cheaper – wire in the central part of the windings where the radial magnetic field is negligible. The proposed windings with different configurations are illustrated in Fig. 9. In Conf. #1 (Conf. is abbreviation of configuration), both HV and LV windings are fully wound with Fujikura wire. In Conf. #2, both HV and LV windings are fully wound with Shanghai Superconductor wire. In Conf. #3, the hybrid configuration, four discs of the end parts of both the HV and LV windings are wound with Fujikura wire while the rest of the windings are wound with Shanghai Superconductor wire.

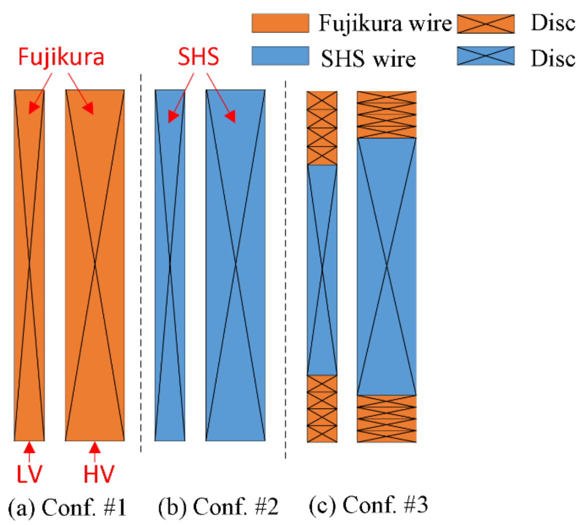

Fig. 9. Schematics of hybrid transformer windings: (a) Conf. #1, (b) Conf. #2, (c) Conf. #3. Here, Conf. means configurations.

Table 3. Loss in transformer windings having different configurations.

Configuration	Conf. #1	Conf. #2	Conf. #3
Loss in transformer winding (kW)	3.79	4.06	3.82

Table 3 compares the simulated loss values in the three winding configurations. AC loss in the transformer windings for Conf. #1 (high performance wire) is the lowest, for Conf. #2 (low performance wire) is the highest and drops to almost the same value as the high-performance case for Conf. #3 (hybrid configuration). The AC loss in the HV and LV windings shows the same tendency. The difference in AC loss values between Conf. #1, (high performance wire) and Conf. #2 (low performance wire) is 7% due to the difference in $I_c(B)$ performance of the wires. However, the difference in AC loss values between Conf. #1 (high performance wire) and Conf. #3 (hybrid configuration) is only 2%, even though the hybrid configuration uses only a small fraction of the high-performance wire in the end of the windings. The result indicates the effectiveness of the hybrid winding approach for wire cost reduction of traction transformers.

3.5 Flux diverters at the winding ends reduce AC loss

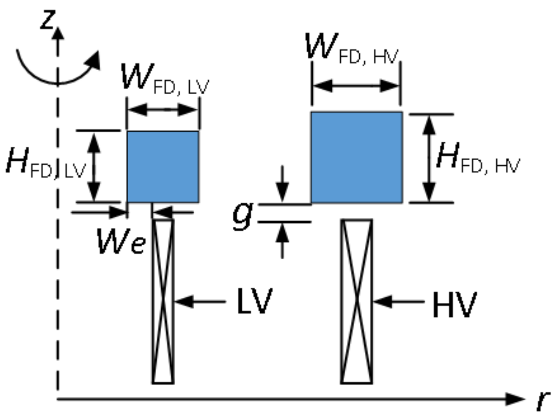

Fig. 10. Quarter model of the placement of flux diverters at the ends of HV and LV windings. For clarity, the figure is not drawn to scale.

We also investigated how flux diverters will affect the magnetic flux distribution for the HV and LV windings. Two flux diverters were considered near the outer ends of the HV and LV windings, as shown in Fig. 10. The dimensions of the flux diverters for the HV and LV windings are denoted by $H_{FD,\ HV}$, $W_{FD,\ HV}$, $H_{FD,\ LV}$, and $W_{FD,\ LV}$, respectively. W_e is the distance by which the flux diverter overhangs both the inner and outer radius of the winding and g is the gap between the end of the windings and the flux diverters. Two flux diverters (FD1 and FD2) with dimensions listed in Table 4 were designed to explore their influence on AC loss. Note that the flux diverter used in this paper was considered a powdered NiFe alloy material with a saturation flux density of 1.5 T and AC loss in the powdered flux diverters is negligible [9].

Table 4. Specifications of flux diverters.

Symbol	FD1	FD2
We (mm)	1	8
g (mm)	0.5	0.5
WFD, HV (mm)	6.2	20.2
HFD, HV (mm)	6.2	6.2
WFD, LV (mm)	3.8	17.8
HFD, LV (mm)	3.8	3.8
μ_r	100	100

The AC loss in L1 transformers using FD1 and FD2 is shown in Table 5. AC loss in the transformer is significantly decreased using flux diverters compared to that without flux diverters. AC loss with greater W_e

leads to smaller AC loss [7]. With FD2, the AC loss in the L1 transformer becomes slightly lower than the 2 kW target of this project.

Table 5. Loss in transformer windings different flux diverters

	Without flux diverters	FD1	FD2
Loss in transformer winding (kW)	3.79	2.89	1.93

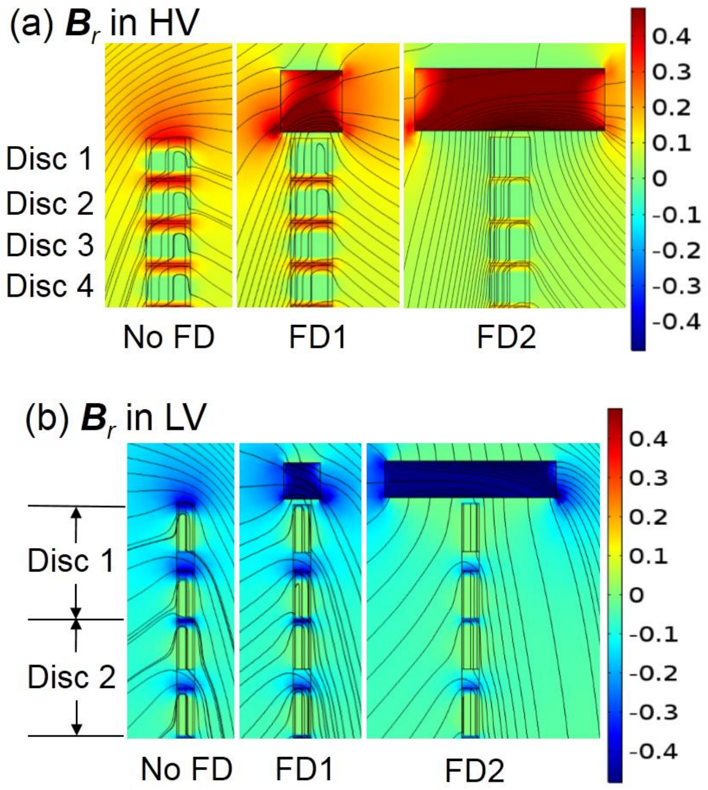

Fig. 11. Distribution of radial magnetic field and magnetic flux lines in the 6.5 MVA transformer designed with different flux diverters: (a) HV winding, (b) LV winding.

Fig. 11 shows the distribution of B_r in the HV and LV windings with and without flux diverters. Both the magnitude of B_r and the area filled with large B_r are larger in the transformer windings without flux diverters compared to those with flux diverters. Furthermore, the magnetic field is more perpendicular in the discs in the transformer windings without flux diverters. With increasing W_e, the magnetic field around the discs becomes more parallel and the high field region diminishes in extent. On the other hand, we can see more concentration of magnetic field inside the flux diverters with increasing W_e. The result clearly shows the effectiveness of flux diverters for reducing AC loss in the transformer windings by shaping the magnetic field around the transformer windings.

3.6 Harmonics can increase AC loss

Harmonic content in the transformer output has the potential to significantly increase the AC loss beyond that associated with the fundamental sinusoid [7]. Because AC loss is hysteretic, the loss is proportional to frequency, and so the higher frequency harmonics can contribute a proportionately greater AC loss. Harmonic content will however only produce extra AC loss if it causes extra reversals of the direction of flux penetration of the conductor during the power cycle, in other words, if there are multiple peaks of current flow during each half cycle. For example, a sawtooth or a square waveform will produce exactly the same AC loss as a sinusoidal waveform of the same amplitude and frequency even though these non-sinusoidal waveforms have substantial harmonic content. The PWM converters for traction motors have the potential to draw current with large harmonic content; the challenge is to control the current waveform so it does not produce significant harmonic AC loss.

4. Cooling system

The basic requirement for the cooling system is to provide 2.5 kW of cooling power at a temperature range of 65 – 67 K. The 2.5 kW cooling power allows for 2.0 kW of AC loss and 0.5 kW of heat leak from the cryostats and current leads (estimated at 43 W heat leak per kA of lead current). The concept design has the windings enclosed in epoxy fiberglass composite cryostats, one for each pair of winding units on each leg of the transformer core. The cryostats are constructed of non-conductive composite because the transformer core is at room temperature so the cryostats must encircle the legs of the core without providing a shorted turn. A metal cryostat can be used if the iron core is completely enclosed within it, as in the Siemens traction transformer [3], but then all the core dissipation of around 1 kW would be added to the load on the cooling system. This thermal load and consequent added weight are avoided by having a warm iron core and composite cryostats. Ideally the transformer would have a stand-alone closed-loop cooling system using an on-board cryocooler. However, cryocoolers which could provide the required cooling power within the weight and space constraints of the project are not commercially available. The closest match to requirements is the Stirling SPC-4 cryocooler, providing 2.8 kW of cooling power at 65 K, but this will not fit in the available space. Moreover, the total cost of ownership of this cooler, at over 300 USD/W of cooling power [10], though better than alternatives, is forbidding. Lacking a viable cryocooler option, the alternative is an open-loop system using pumped cooling from an on-board liquid nitrogen storage tank.

This has the disadvantage that it would entail providing liquid nitrogen filling facilities at terminals. However, this is perhaps no greater handicap than the need to provide refuelling facilities for diesel locomotives.

In terms of cooling power and operating temperature the requirements for the traction transformer are similar to those of the open-loop cooling system for the Ampacity superconducting cable that has been operating in Essen, Germany, since 2014 [11]. For the traction transformer, we need to cool a compact winding instead of a km-long cable. We can reduce the weight and complexity of the cable cooling system by bringing the sub-cooler inside the cryostat as shown in Fig. 12. This compact system has been demonstrated in a fault current limiting transformer demonstration [6]. Natural convection is used to transfer heat from the windings to the sub-cooler/heat exchanger.

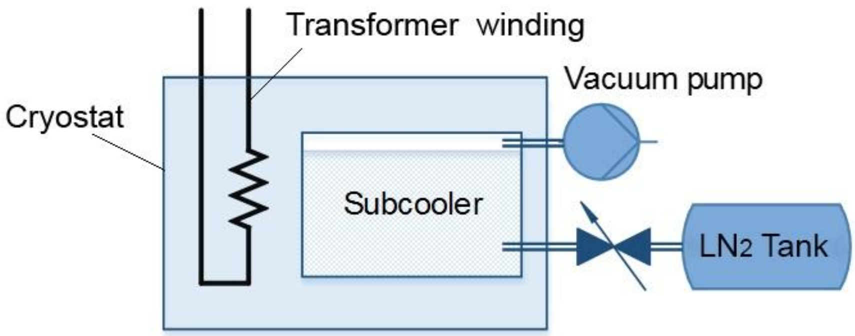

Fig. 12. Schematic of traction transformer cooling system. The subcooler / heat exchanger is immersed in the sub-cooled liquid nitrogen in each cryostat.

Can we provide the required cooling power and carry enough liquid nitrogen on-board for travel between terminals within the weight constraints? Assuming a typical storage dewar pressure of 3 bar, the rate of liquid nitrogen consumption per unit cooling power at 65 K can be estimated to be 20.5 kg/kWh from standard specific entropy values.

Table 6. Weight of the transformer system components, assuming two values of required cooling power, 2.5 and 5 kW, and assuming a running time of 8 hours before refilling the on-board nitrogen storage tank.

Cooling power (kW)	2.5		5	
LN_2 storage vessel	255	9%	404	11%
LN_2 in storage	410	14%	820	23%
Claw vacuum pumps	230	8%	460	13%
Cryostats	171	6%	171	5%
LN_2 in cryostats	452	16%	452	12%
Wire, formers, etc.	96	3%	96	3%
Core	1223	43%	1223	34%
Total for system	2847 kg	100%	3639 kg	100%

.

Table 6 summarizes the total weight of the transformer system and its components for two assumed values of cooling power. Note that these estimates are based on a concept design, and may be subject to change as the detailed design is developed. For 2.5 kW cooling power the total weight comes in comfortably below the 3000 kg target, but for 5 kW the target is exceeded by more than 20%, underlining how important low loss in the transformer is for constraining the system weight. For 2.5 kW cooling power the cooling system – stored nitrogen and pumps – contributes 31% of total weight, the transformer 46%, and the cryostat and nitrogen charge (the equivalent of the tank and oil in a conventional transformer) 22% of the total. The weight to cooling power ratio of the 2.5 kW system is about 360 kg/kW. This is somewhat lighter than the Stirling SPC-4 cryocooler alternative (410 kg/kW cooling power at 65 K) but the major advantages of the open-loop system lie more in cost, reliability, provision of redundancy, and flexible layout of components to fit within the space allocated for the transformer system.

5. Conclusion

The CRRC Fuxing train power system is currently limited by the size, weight and rating of the traction transformer supplying the variable speed drive to the electric traction motors. A significant part of the size and volume is used by the cooling system required to overcome the electrical losses in a conventional transformer. The models, calculations and designs show that the use of high temperature superconductors can significantly reduce traction transformer system mass and volume.

We showed that the existing 6.5 MVA traction transformers can be replaced with drop-in superconducting transformers which can achieve 50% (3 tons) mass reduction and a 4.5% efficiency gain to 99.5% efficiency. This allows either higher power systems, greater passenger volumes or higher speeds to be attained with the existing train design.

This superb outcome is only possible through the minimization of AC loss in the HTS windings. We showed that the use of modern high-performance wire, high current HTS Roebel cable, high aspect-ratio windings, and flux diverters placed at the winding ends all contribute to reducing the electrical loss to less than 2 kW. We also demonstrated that the use of hybrid superconducting windings can achieve a significant performance advantage whilst optimizing costs.

The project has progressed to design review; the electromagnetic design has been peer-reviewed and accepted by CRRC Corporation Limited as meeting the technical requirements of the application. The prototype is now progressing through the manufacture of individual components and subsystems into assembly and factory acceptance testing to CRRC performance requirements. The certified transformer will finally be installed in a Fuxing high-speed train for an in-service evaluation programme.

References

[1] IEA Technology Report, “The future of rail,” IEA, Paris, 2019, https://www.iea.org/reports/the-future-of-rail.

[2] https://www.eesi.org/papers/view/fact-sheet-high-speed-rail-development-worldwide#3.

[3] M. Meinert, M. Leghissa, R. Schlosser, et al., “System test of a 1-MVA-HTS-transformer connected to a converter-fed drive for rail vehicles,” IEEE Transactions on Applied Superconductivity, vol. 13, no. 2, pp. 2348-2351, 2003.

[4] H. Kamijo, H. Hata, H. Fujimoto, et al., “Fabrication of inner secondary winding of high-T_c superconducting traction transformer for railway rolling stock,” IEEE Transactions on Applied Superconductivity, vol. 15, no. 2, pp. 1875-1878, 2005.

[5] N. Glasson, M. Staines, Z. Jiang, and N. Allpress, “Verification testing for a 1 MVA 3-phase demonstration transformer using 2G-HTS Roebel cable,” IEEE Transactions on Applied Superconductivity, vol. 23, no. 3, art. no. 5500206, 2013.

[6] M. Yazdani-Asrami, M. Staines, G. Sidorov, et al., “Fault current limiting HTS transformer with extended fault withstand time,” Superconductor Science and Technology, vol. 32, art. no. 035006, 2019.

[7] W. Song, Z. Jiang, M. Staines, et al., “Design of a single-phase 6.5 MVA/25 kV superconducting traction transformer for the Chinese Fuxing high-speed train,” International Journal of Electrical Power & Energy Systems, vol. 119, art. no. 105956, 2020.

[8] W. Song, Z. Jiang, M. Staines, et al., “AC loss calculation on a 6.5 MVA/25 kV HTS traction transformer with hybrid winding structure,” IEEE TransActions on Applied Superconductivity, vol. 30, no. 4, art. no. 5500405, 2020.

[9] S. You, M. Staines, G. Sidorov, D. Miyagi, R. A. Badcock, N. J. Long and Z. Jiang, “AC loss measurement and simulation in a REBCO coil assembly utilising low - loss magnetic flux diverters,” Superconductor Science and Technology, vol. 33, art. no. 115011, 2020

[10] M. Staines, E. Pardo, L. Jolliffe, M. Pannu, and N. Glasson, “Prospects for HTS transformers in the grid: AC loss and economics,” Poster presentation at EUCAS 2015, https://www.wgtn.ac.nz/robinson/research/publications/publications/Staines_EUCAS2015.pdf.

[11] F. Herzog, T. Kutz, M. Stemmle, and T. Kugel, “Cooling unit for the AmpaCity project – One year successful operation,” Cryogenics, vol. 80, no. 2, pp. 204-209, 2016.

Acknowledgement

This work was supported by the Chinese Ministry of Science and Technology through the National Key Research and Development Program of China under Grant No. 2016YFE0201200. The authors acknowlege Gennady Sidrov for producing figures for cooling system.

Authors

Wenjuan Song (Member, IEEE) received the M.Eng and the Ph.D. degrees in Electrical Engineering from Beijing Jiaotong University (BJTU), China, in 2015 and 2019, respectively.

She was a visiting researcher/research assistant in Robinson Research Institute, Victoria University of Wellington, New Zealand for more than two years from 2016 to 2018. Since 2019, she joined as a postdoctoral research associate in Department of Electronic & Electrical Engineering at University of Bath. Her field of expertise is electromagnetic analysis for superconducting power applications, AC loss calculation and measurement of superconductors, design and development of superconducting fault current limiters and transformers.

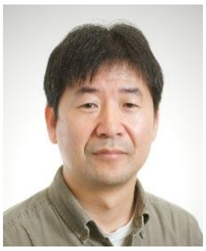

Zhenan Jiang received a B.Eng. in Electrical Engineering from Chongqing University in Chongqing, China in 1994, and M. Eng., Ph.D. Eng. in applied superconductivity from Yokohama National University in Yokohama, Japan in 2002 and 2005, respectively.

He was a Postdoctoral Research Fellow at Yokohama National University from 2005 to 2008. He joined the Superconductivity Group currently known as the Robinson Research Institute, Victoria University of Wellington, New Zealand in 2008 as Research Scientist. He is Principal Scientist at the same institute. He has authored in more than 100 peer reviewed journal papers (36 first author papers) with an *h* – index of 26 and more than 2250 citations. His recent research interests include AC loss characterization in HTS coils, HTS flux pumps and rotating machines as well as HTS transformer/magnet applications.

He has been twice awarded the JSPS (Japan Society for the Promotion of Science) invitation fellowship to Kyoto University in 2011 and 2015, respectively. He is a visiting professor and foreign expert of Beijing Jiaotong University, China.

Mike Staines completed his PhD in physics in 1979 and has been engaged in high temperature superconductor research since 1987, working mostly in superconducting wire development and measurement of electrical properties, particularly AC loss, of HTS wire, cable, and windings.

Transformer work has included the development of a 3-phase 1 MVA HTS transformer, a fault current limiting 45 kVA transformer, cost-effective transformer cooling systems, and quantifying the value proposition for HTS transformers.

Stuart Wimbush is a Principal Scientist at the Robinson Research Institute of Victoria University of Wellington with longstanding expertise in superconducting materials and applications. He was awarded the Dr. rer. nat. degree in Physics by the TU Dresden, Germany, in 2004, and has worked previously as an Independent Research Fellow at the National Institute for Materials Science, Japan, and as a Senior Research Fellow at the University of Cambridge, UK. Dr Wimbush is a Chartered Physicist and Fellow of the Institute of Physics, as well as a Senior Member of the IEEE.

Jin Fang received his Ph.D from the Institute of Plasmas, Chinese Academy of Sciences in 2002. His major is condensed matter physics. His research topics include design, stability and AC losses of superconducting materials, cables and superconducting magnets. In 2002, he joined the Department of Physics of Tsinghua University for postdoctoral research, and mainly engaged in basic application research of high temperature superconducting tapes. In 2004, he joined Beijing Jiaotong University to carry out research on power transmission cables, superconducting magnetic levitation technology, superconducting linear motors, and power system simulation. Dr. Jin Fang has been awarded a NZ Catalyst Leaders funding of the Royal Academy of Sciences (2018-2021). He published more than 100 papers on superconductivity including more than 50 SCI papers. Five patents have been awarded for the invention of HTS linear induction motors.

Jinping Zhang received Bachelor Degree of Motor and Electromagnetism from Taiyuan University of Technology in1991 and a Master Degree of Engineering from Beijing Jiaotong University in 2003. He has more than 28 years Traction Transformer experience in the railway industry. He specialized in the technology in the field of traction transformers of EMU (electrical multiple unit) and locomotives. He is familiar with the general structure of electrical locomotives and EMU. He has designed more 2000 units of Traction Transformer for locomotive and EMU trains. He held multiple roles in engineering, sales and management in ABB and Bombardier.

Rodney A. Badcock (SM'18) received the B.Sc. degree in physics with electronics from the University of Leeds, Leeds, U.K., and the M.Sc. and Ph.D. degrees in manufacturing and materials engineering from Brunel University, England, U.K. He has 30 years research experience in applied R&D covering manufacturing process monitoring and control, materials sensing, and superconducting systems. Since 2006, he has concentrated on superconducting machines, and production and machines for General Cable Superconductors at the Robinson Research Institute, Victoria University of Wellington, Lower Hutt, New Zealand. He is currently the Institute Deputy Director, Chief Engineer, Professor and specializes in the management of complex engineering projects, including customer-focused multidisciplinary projects. He is particularly known for the development of the superconducting dynamos for electric machines and the NZ MBIE programme developing aircraft superconducting electric propulsion technology. Rod is recognized as one of the leading experts in the application of superconducting dynamos and cables to electric machines.

Dr. Badcock was a key member of the team awarded the Royal Society of New Zealand Cooper Medal in 2008 for the development of high-temperature superconducting cables for power system applications including 1 MVA transformer, 60 MW hydro generator, and 150 MW utility generator.